Human Pathology (2019) **83**, 159–165

ELSEVIER

Human PATHOLOGY

www.elsevier.com/locate/humpath

Original contribution

Histologic findings associated with false-positive multiparametric magnetic resonance imaging performed for prostate cancer detection☆,☆☆

Jennifer B. Gordetsky MD[a,b,*], David Ullman MD[a], Luciana Schultz MD[c], Kristin K. Porter MD[d], Maria del Carmen Rodriguez Pena MD[a], Carli E. Calderone MD[b], Jeffrey W. Nix MD[b], Michael Ullman MD[e], Sejong Bae PhD[f], Soroush Rais-Bahrami MD[b,d]

[a]*Department of Pathology, University of Alabama at Birmingham, Birmingham, AL 35249, USA*
[b]*Department of Urology, University of Alabama at Birmingham, Birmingham, AL 35249, USA*
[c]*Instituto de Anatomia Patológica, Piracicaba, Santa Bárbara d'Oeste 13419-160, Brazil*
[d]*Department of Radiology, University of Alabama at Birmingham, Birmingham, AL 35249, USA*
[e]*MedStar Georgetown University Hospital, Washington, DC 20007, USA*
[f]*Division of Preventive Medicine, University of Alabama at Birmingham, Birmingham, AL 35249, USA*

Received 20 June 2018; revised 17 August 2018; accepted 23 August 2018

Keywords:
Multiparametric MRI;
Prostatitis;
Prostate biopsy;
False-positive imaging;
Pathology;
Histology;
Cancer

Summary Magnetic resonance imaging (MRI)/ultrasound fusion–targeted biopsy (TB) has been shown to more accurately identify higher-grade prostate cancers compared with standard-of-care systematic sextant prostate biopsy (SB). However, occasional false-positive imaging findings occur. We investigated the histologic findings associated with false-positive prostate MRI findings. A retrospective review was performed on our surgical pathology database from 2014 to 2017 selecting patients with no cancer detected on TB with concurrent SB after at least 1 prior benign SB session. Histologic features evaluated included percentage of core involvement by chronic inflammation, percentage of core composed of stroma, percentage of glands involved by atrophy, and presence of the following features: acute or granulomatous inflammation, stromal nodular hyperplasia, adenosis, squamous metaplasia, basal cell hyperplasia, and presence of skeletal muscle. Histologic findings were compared between TB and concurrent SB. We identified 544 patients who underwent TB. Of these, 41 patients, including 62 targeted lesions, met criteria. Compared with SB tissue, the mean percentage of stroma was increased in TB ($P = .02$). Basal cell hyperplasia was also found to be more common on TB ($P = .02$). Both high percentage of stroma ($P = .046$) and presence of basal cell hyperplasia ($P = .038$) were independent predictors on multivariate analysis. The combination of high chronic inflammation, high stroma, acute inflammation, and basal cell hyperplasia was associated with TB ($P = .001$).

☆ Competing interest: Jeffrey W. Nix and Soroush Rais-Bahrami serve as consultants for Philips/InVivo Corp. All other authors report no conflicts of interest or financial disclosures that were pertinent to this study.

☆☆ Funding/Support: This work was funded by a Junior Faculty Development Grant (ACS-IRG 001-53) and by developmental funds from the UAB Comprehensive Cancer Center Support Grant (NCI P30 CA 013148) to Soroush Rais-Bahrami, MD.

* Corresponding author at: Department of Pathology, University of Alabama at Birmingham, NP 3550, 1802 6th Avenue South, Birmingham, AL 35249.
E-mail address: jgordetsky@uabmc.edu (J. B. Gordetsky).

https://doi.org/10.1016/j.humpath.2018.08.021

Atrophic glands and chronic inflammation showed a positive correlation ($r = 0.67$, $P = .003$), which was especially seen in high prostate imaging reporting and data system lesions. Specific benign histologic entities are associated with false-positive findings on prostate MRI.

1. Introduction

Historically, prostate cancer has been difficult to identify on imaging. Although transrectal ultrasound (US) was used to guide placement of the biopsy needle, it did not accurately localize lesions suspicious for malignant disease. Thereby, detection of prostate cancer classically depended on systematic sampling of the prostate gland using a sextant approach. These biopsies represented a random tissue sampling rather than biopsies targeting a specific lesion suspicious for harboring cancer. To date, prostate cancer remains the only solid organ malignancy standardly diagnosed in this fashion.

Magnetic resonance imaging has shown improvement in the identification of prostate cancer on imaging. Indeed, studies have shown equivalent detection of prostate cancer using an MRI/US fusion–targeted biopsy (TB) approach compared with the systematic extended-sextant biopsy (SB) technique while limiting the number of cores sampled [1-3]. TB has also been shown to detect more clinically significant cancers [4-6]. This has been shown in patients undergoing initial biopsy for clinical suspicion of prostate cancer as well as men who have had a prior negative standard biopsy [7].

Despite the optimization in prostate cancer detection, there remain limitations to this new technology. One of these limitations is the presence of false-positive lesions identified as suspicious for malignancy on MRI. Studies have shown that there are certain entities that can lead to false-positive reads on MRI. Some examples include inflammation, glandular hyperplasia, and stromal hyperplasia [8-12]. However, understanding the histologic findings behind false-positive MRI findings for the detection of prostate cancer is still being explored. Herein, we investigate benign prostate gland histology associated with false-positive lesions on prostate MRI.

2. Materials and methods

A retrospective institutional review board–approved search was performed on our surgical pathology database from 2014 to 2017. Image processing and targeting of lesions at the time of biopsy was performed using the DynaCad software and UroNav fusion biopsy system, respectively (Phillips/InVivo Corp, Gainsville, FL). Prostate imaging reporting and data system (PIRADS) version 2 scoring was assigned by a multidisciplinary consensus conference with fellowship-trained radiologists and urologic oncologists specializing in prostate MRI, all with more than 4 years of experience with prostate MRI. Two fellowship-trained urologic oncologists performed all TBs. Each targeted lesion was sampled by at least 2 needle cores as recommended based on prior publication [13]. Patients were selected that had no history of prostate cancer and at least 1 previous SB session. Patients were then filtered for those who underwent an additional biopsy session with TB and concurrent repeat SB with all cores negative for adenocarcinoma. As patients underwent concurrent TB and SB, each patient was able to act as their own control for the purposes of analyses performed comparing TB tissue with SB tissue.

Prostate tissue sampled was organized by sextants. Tissue from the area of the TB was compared with a section of tissue from a SB taken during the same biopsy procedure that was separated by at least 2 sextants (Fig. 1). Patients were limited to those who had a maximum of 2 targeted lesions on TB to allow for enough sextant distance between the standard and targeted tissue cores. Histologic features were evaluated including the percentage of tissue involvement by chronic inflammation, the percentage of tissue composed of stroma, and the percentage of glands involved by atrophy. A high

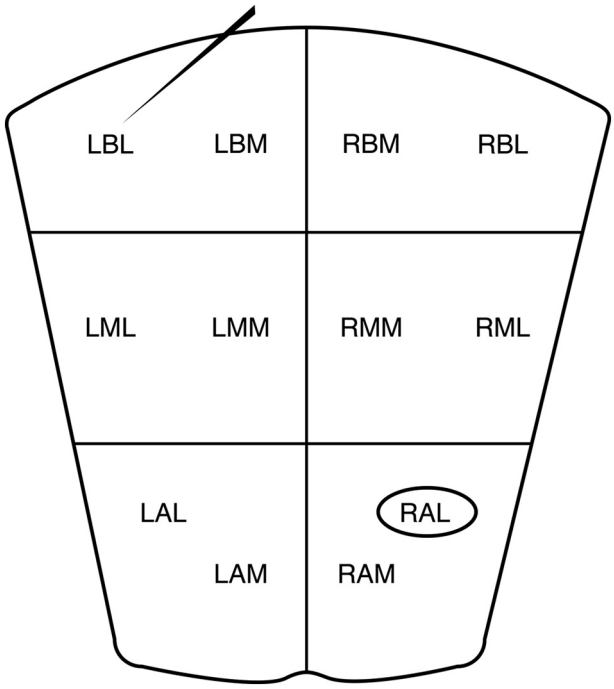

Fig. 1 Prostate gland extended-sextant template with a needle representing tissue examined from a TB site and a circle representing comparative tissue examined from a standard biopsy site at least 2 quadrants from the targeted lesion.

degree of chronic inflammation was defined according to a cutoff of 10% of tissue involved. A high degree of stroma was defined according to a cutoff of 60% of tissue involved. In addition, the presence or absence of the following features was assessed: acute inflammation, granulomatous inflammation (necrotizing or nonspecific granulomatous prostatitis), stromal nodular hyperplasia, adenosis, squamous metaplasia, basal cell hyperplasia, and skeletal muscle. Histologic findings on TB were compared with SB. Additional clinical and radiologic information was gathered, including patient age, prostate-specific antigen (PSA), and corresponding PIRADSv2 score for each targeted lesion detected on MRI (Fig. 2). Evaluation of all prostate biopsy pathology was performed by 2 urological pathologists (J. B. G. and L. S.).

Statistical analyses were done using STATA (StataCorp 2005. Stata Statistical Software: Release 9.2; StataCorp, College Station, TX). The χ^2 test was used for categorical variables and Student *t* test for continuous variables. Categorical and continuous variables were compared using Kruskal-Wallis 1-way analysis of variance. Linear dependences were calculated using the Spearman correlation.

3. Results

We identified 544 patients who underwent MRI/US TB. Of these, 96 patients had no tumor on TB and concurrent 12-core extended-sextant SB. Of this cohort, 75 patients had a maximum of 2 targeted lesions on MRI for appropriate separation of tissue. Of these, 47 patients had at least 1 prior negative SB session. From this group, a final cohort of 41 patients had concurrent SB tissue at least 2 sextants away from the concurrent TB. The mean number of previous negative SB for our final cohort was 1.6 (range, 1-5). Since the time of the concurrent TB with SB, 3 patients underwent an additional follow-up prostate biopsy, all negative for prostatic adenocarcinoma.

Tissues from 62 targeted lesions were compared with tissues from 41 SBs (Table 1). The mean PSA was 8.5 ± 4.2 ng/mL, and the mean age was 63.2 ± 6.2 years. Mean PIRADS score was 3.3 ± 0.7. Twenty-one (51.2%) of 41 patients had 1 targeted lesion. The remaining 20 (48.8%) of 41 patients had 2 targeted lesions. The mean number of targeted cores biopsied per patient was 3.4 ± 1.2. In terms of location of the

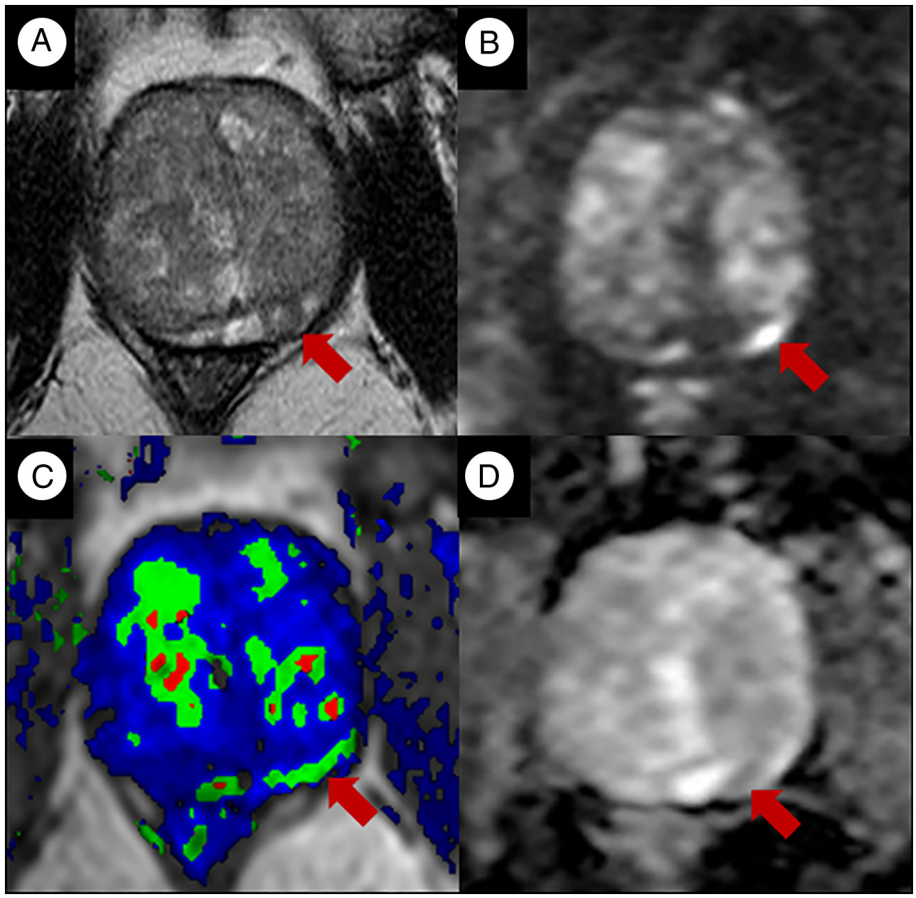

Fig. 2 Left posterior mid-gland peripheral zone focal moderate hypointensity on ADC (red arrow, D) with corresponding mild hyperintensity on high *b*-value diffusion-weighted image (red arrow, B) corresponds to a circumscribed moderate hypointense focus on T2-weighted images (red arrow, A). There is also asymmetric perfusion (red arrow, C). This lesion is high suspicion for clinically significant prostate cancer (PIRADS 4).

Table 1 Patient clinical and imaging characteristics

Patient characteristic	n	%
Race		
African American	5	12
White	24	59
Unknown	12	29
Age (y)		
51-60	15	36
61-70	22	54
71-80	4	10
Mean, 63.2 ± 6.2 y		
PSA		
<10	31	76
>10.1	10	24
Mean, 8.5 ± 4.2 ng/mL		
Targeted lesions per patient		
1 lesion	21	51.2
2 lesions	20	48.8
PIRADS		
I	2	3
II	12	19
III	31	50
IV	16	26
V	1	2
Mean, 3.3 ± 0.7		

targeted lesions, 32 (51.6%) of 62 lesions were located in the right lobe and 30 (48.4%) of 62 in the left lobe. Lesions were most common in the mid-gland (25/62 [40.3%]) followed by the base (21/62 [33.9%]) and apex (16/62 [25.8%]). The posterior gland (44/62; 71%) was more common than the anterior gland (18/62 [29%]), and the peripheral zone (38/62 [61.3%]) was more common than the central zone (24/62 [38.7%; Table 2).

TB tissue, as examined in this patient cohort, had increased mean percentage of stroma compared with SB tissue (67.0% versus 59.4%, respectively; $P = .02$; Table 3). In addition, high percentage of stroma remained an independent predictor of TB tissue over SB tissue on multivariate analysis ($P = .046$). Basal cell hyperplasia was also more frequent in TB tissue compared with SB tissue (13/62 [21.0%] versus 2/62 [3.2%], respectively; $P = .02$). This finding maintained statistical significance on multivariate analysis ($P = .038$; Table 4). Acute inflammation was also increased in TB tissue (18/62 [29.0%] versus 6/41 [14.6%]), which trended toward statistical significance ($P = .09$). TB tissue had increased mean percentage of chronic inflammation compared with SB tissue (10.3% versus 7.1%); however, this was not statistically significant ($P = .14$). The presence of skeletal muscle was not significantly different between the 2 groups, seen in 7 (17.5%) of 41 SBs and 10 (16.1%) of 62 TBs ($P = .90$). Presence of granulomatous inflammation was not statistically different between the 2 groups, seen in 1 (2.5%) of 41 SBs and 2 (3.2%) of 62 TBs ($P = .82$). Similarly, differences in squamous metaplasia were not significant, seen in 1 (2.5%) of 41 SBs and 3 (4.8%) of 62 TBs ($P = .53$). Stromal nodular hyperplasia was only found in 2 cases and was present only on TB tissue from those cases ($P = .25$). Adenosis was only found in 2 cases, both identified in the TB tissue cores ($P = .25$). Both of these lesions had a high PIRADSv2 score of 4. Atrophic glands and chronic inflammation showed a positive correlation among all lesions ($r = 0.39$, $P < .0001$) and correlated more strongly among lesions with high PIRADS suspicion scores ($r = 0.66$, $P = .0034$). We found that the combination of high chronic inflammation, high percentage of stroma, presence of acute inflammation, and presence of basal cell hyperplasia correlated with TB tissue ($P = .001$; Figs. 3 and 4).

Table 3 Histologic features comparing targeted prostate biopsy tissue suspicious for cancer on MRI with standard biopsy tissue

	Targeted biopsy (%)	Standard biopsy (%)	*P*
Percentage of stroma	67.0	59.4	.02
Basal cell hyperplasia	21.0	3.2	.02
Acute inflammation	29.0	14.6	.09
Chronic inflammation	10.3	7.1	.14
Granulomatous inflammation	3.20	2.50	.82
Skeletal muscle	16.1	17.5	.90
Squamous metaplasia	4.80	2.50	.53

Table 2 Location of targeted lesions

Location	n	%
Right	32	51.6
Left	30	48.4
Base	21	33.9
Mid	25	40.3
Apex	16	25.8
Anterior	18	29
Posterior	44	71
Central	24	38.7
Peripheral	38	61.3

Table 4 Multivariate analysis predicting benign targeted biopsy tissue suspicious for cancer on MRI

Parameter	Odds ratio	95% Confidence limits		*P*
High chronic inflammation	1.616	0.561	4.651	.3735
Acute inflammation	0.535	0.178	1.61	.2659
Basal cell hyperplasia	5.369	1.095	26.327	.0383
High stromal component	2.386	1.016	5.601	.0459

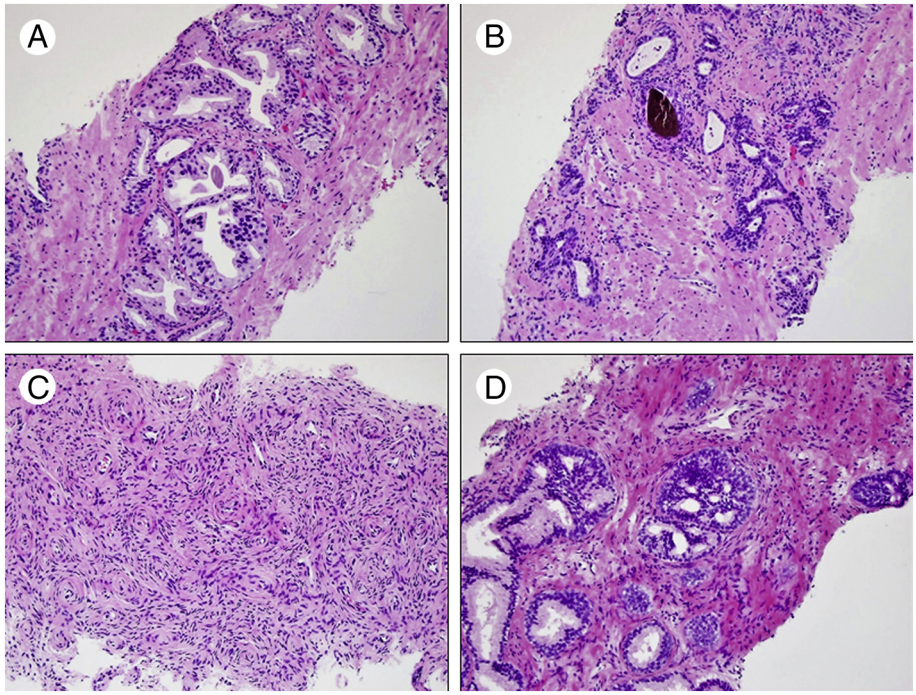

Fig. 3 Hematoxylin-eosin–stained slides of prostate core biopsy tissue showing benign prostate glands with a typical gland-to-stroma ratio (A), atrophic prostate glands with increased stroma (B), stromal nodular hyperplasia (C), and basal cell hyperplasia (D).

4. Discussion

Multiple studies have shown the superiority of multiparametric MRI and MRI/US fusion-targeted biopsies over the standard-of-care extended-SB approach in the detection of clinically significant prostate cancer. Indeed, TB is now recommended for patients with a prior negative SB and continued clinical suspicion for prostate cancer, including elevated PSA [7,14]. In addition, MRI/US TB has been shown to be useful in other situations, such as patients on active surveillance [15]. With the growing acceptance and utilization of this technology, more patients will become candidates for TB. To date, most patients who undergo MRI/US TB are not biopsy naïve. In other words, they have previously undergone a SB, and they had either a benign pathology result or they are pursuing active surveillance [16]. Many previous studies evaluating the utility of MRI in the diagnosis of prostate cancer have focused on the high negative predictive value of this technique. Having a low false-negative rate is logically of utmost importance so as not to miss cases of clinically significant cancer. However, achieving a very low false-negative rate comes with the inevitable problem of false-positive imaging suspecting prostate cancer, which is not detected on biopsy sampling. Our goal as a part of this study was to help define the pathologic causes of false suspicion on prostate MRI to ultimately help guide methods of reducing the number of unnecessary biopsies.

It has previously been shown that MRI can result in false-positive imaging results when using this technique for the detection of cancer in different organs. For example, in screening for breast cancer, MRI added to mammography can increase the screening sensitivity for women at high risk for malignancy [17]. However, the false-positive rates are also increased using this method. Similarly, MRI has been studied for the detection for pulmonary nodules representing lung cancer, but again, a significant number of false-positive diagnoses were observed [18]. A similar phenomenon has been described in MRI used for prostate cancer screening. In general, the stroma of the anterior prostate gland and of central zone have low signal on T2-weighted MRI, mimicking prostate cancer [11]. However, contrary to this phenomenon, we found that most of our suspicious lesions with benign pathology were present in the posterior aspect of the gland and the peripheral zone. In addition, although benign prostatic hyperplasia typically has increased T2-weighted signal, stromal nodular hyperplasia can mimic transition zone tumors [11]. Furthermore, inflammation can present as a lesion on MRI suspicious for prostate cancer. We previously described granulomatous prostatitis presenting as lesions highly suspicious for prostate cancer (PIRADSv2 scores 4 and 5) [8]. Other studies have demonstrated that prostatitis can appear similar to prostate cancer with low signal intensity on T2-weighted images and early enhancement on contrast-enhanced MRI [9,10]. Interestingly, in our current study, we did not find a difference between TB tissue and SB tissue in terms of granulomatous inflammation. However, this is likely due to the small number of cases (n = 3) with granulomatous inflammation present in our study population.

Diffusion-weighted MRI depends on the movement of water molecules in tissue. The restriction of diffusion, which can be caused by any increase in cellularity, results in decreased

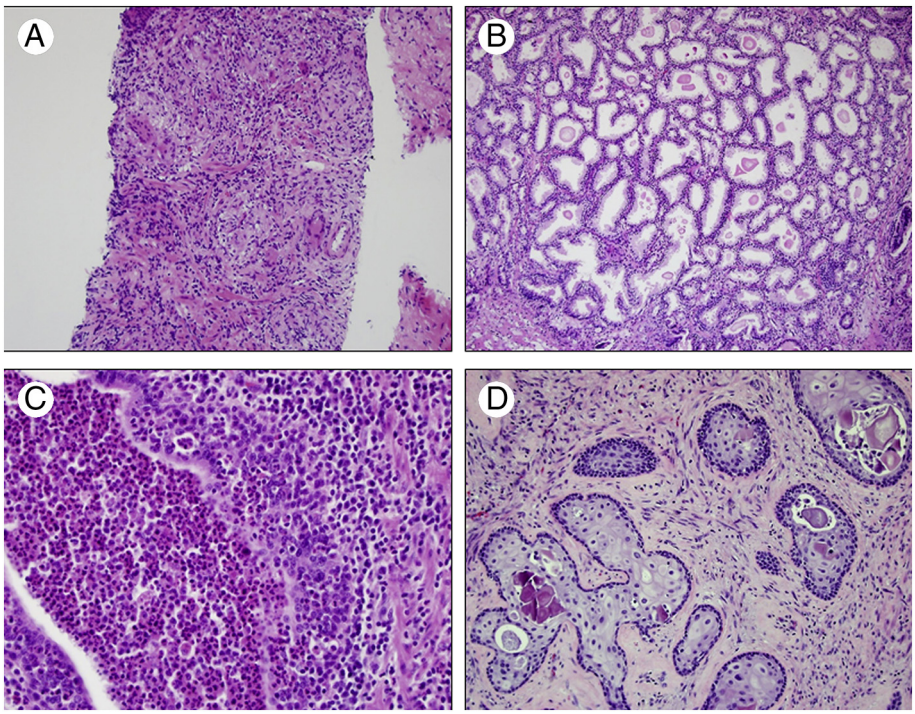

Fig. 4 Hematoxylin-eosin–stained slides of prostate core biopsy tissue showing nonspecific granulomatous prostatitis (A), adenosis (B), acute inflammation (C), and squamous metaplasia (D).

signal. Thus, prostate cancer, which causes increased cellularity due to the increased number of more densely packed glands, reveals altered water diffusion patterns on MRI. However, stromal nodular hyperplasia may also cause increased relative cellularity. In our study, we found that TB tissue had increased mean percentage of stroma compared with tissue examined from SB ($P = .02$). In addition, a high percentage of stroma was an independent predictor of TB tissue on multivariate analysis ($P = .046$). This increase in stromal density partially helps explain the false suspicion for cancer on MRI. Basal cell hyperplasia was also found to be associated with TB tissue and remained an independent predictor on multivariate analysis ($P = .038$). It is possible that the increased cellularity due to basal cell hyperplasia could similarly create an increased suspicion for prostatic adenocarcinoma on MRI. In addition, we found that stromal nodular hyperplasia and adenosis, although small in numbers (n = 4), were only found on TB. The adenosis lesions both had a PIRADS score of 4, highlighting this particular imaging pitfall.

Dynamic contrast-enhanced MRI is another parameter used in the detection of prostate cancer. Prostate cancer shows earlier enhancement and greater signal on dynamic contrast enhanced images [19]. The increased enhancement is thought to be due to increased angiogenesis and nonphysiologic neovascularity associated with tumor tissues. Because inflammatory and other reparative processes can also stimulate vessel growth and promote increased blood flow, this presents another confounding issue for the diagnostic accuracy of MRI. We found that high chronic inflammation and high stroma, in combination with the presence of acute inflammation and basal cell hyperplasia, were correlated with TB over SB ($P = .001$). This is a logical finding in that inflammation could potentially cause an increase in angiogenesis, whereas basal cell hyperplasia and increased stroma could lead to increased tissue density.

One limitation of our study is the possibility of a pathologically false-negative patient included in our tissue analysis. To attempt to limit this possible bias, all patients selected had at least 1 prior negative SB (range, 1-5) as well as an additional negative TB with concurrent repeat SB. It is important that this particular population of patients is evaluated because they represent a select population of men that are undergoing multiple unnecessary surgical procedures with minimal benefit after at least 2 total SB and an additional augmented sampling via TB. Each biopsy poses a small but significant morbidity including patient discomfort, risk for infection, bleeding, and possible hospitalization not to mention the emotional and financial burden on patients and the health care system. Meanwhile, it is estimated that only 3% to 4% of patients will be diagnosed with prostate cancer after 2 negative SBs [20,21]. It is likely that the number of false negatives is even lower after 2 negative SBs and an additional negative TB, which has been shown to have higher detection rates than SB alone [22].

Finally, it may be argued that our population does not represent a true "false-positive" MRI population, as the average PIRADS score for our population was 3.3. Lesions on prostate MRI with a PIRADS score of 3 have been shown to be associated with a low risk for harboring clinically significant prostate

cancer [23]. However, it should be mentioned that these were patients with enough suspicion on imaging to proceed with a TB in a true clinical setting. This is exactly the population that needs to be addressed, as there is a high degree of unnecessary biopsies in hindsight. Future endeavors need to be taken to better delineate imaging markers that are associated with these newly identified histologic mimickers of prostate cancer seen on MRI, given the increased utilization of this imaging modality for the screening of prostate cancer.

5. Conclusions

There are specific benign histologic entities associated with lesions suspicious for prostatic adenocarcinoma on prostate MRI. Increased stroma and basal cell hyperplasia are associated with lesions falsely suspicious for harboring prostatic adenocarcinoma. High chronic inflammation and high stroma, in combination with the presence of acute inflammation and basal cell hyperplasia, correlated strongly with TB. Additional qualitative features and quantitative measures on MRI need to be investigated to help decrease the amount of unnecessary prostate biopsies driven by false-positive imaging findings corresponding to the benign histology identified.

References

[1] Siddiqui MM, George AK, Rubin R, et al. Efficiency of prostate cancer diagnosis by MR/ultrasound fusion–guided biopsy vs standard extended-sextant biopsy for MR-visible lesions. J Natl Cancer Inst 2016; 108:djw039.

[2] Borkowetz A, Platzek I, Toma M, et al. Comparison of systematic transrectal biopsy to transperineal magnetic resonance imaging/ultrasound-fusion biopsy for the diagnosis of prostate cancer. BJU Int 2015;116:873-9.

[3] Ahmed HU, El-Shater Bosaily A, Brown LC, et al. Diagnostic accuracy of multi-parametric MRI and TRUS biopsy in prostate cancer (PROMIS): a paired validating confirmatory study. Lancet 2017;389: 815-22.

[4] Gordetsky JB, Thomas JV, Nix JW, et al. Higher prostate cancer grade groups are detected in patients undergoing multiparametric MRI-targeted biopsy compared with standard biopsy. Am J Surg Pathol 2017;41: 101-5.

[5] Siddiqui MM, Rais-Bahrami S, Turkbey B, et al. Comparison of MR/ultrasound fusion–guided biopsy with ultrasound-guided biopsy for the diagnosis of prostate cancer. JAMA 2015;313:390-7.

[6] Truong M, Rais-Bahrami S, Nix JW, et al. Perineural invasion by prostate cancer on MR/US fusion targeted biopsy is associated with extraprostatic extension and early biochemical recurrence after radical prostatectomy. Hum Pathol 2017;66:206-11.

[7] Kasivisvanathan V, Rannikko AS, Borghi M, et al. MRI-targeted or standard biopsy for prostate-cancer diagnosis. N Engl J Med 2018;378: 1767-77.

[8] Rais-Bahrami S, Nix JW, Turkbey B, et al. Clinical and multiparametric MRI signatures of granulomatous prostatitis. Abdom Radiol (NY) 2017; 42:1956-62.

[9] Nagel KN, Schouten MG, Hambrock T, et al. Differentiation of prostatitis and prostate cancer by using diffusion-weighted MR imaging and MR-guided biopsy at 3 T. Radiology 2013;267:164-72.

[10] Esen M, Onur MR, Akpolat N, et al. Utility of ADC measurement on diffusion-weighted MRI in differentiation of prostate cancer, normal prostate and prostatitis. Quant Imaging Med Surg 2013;3:210-6.

[11] Quon JS, Moosavi B, Khanna M, et al. False positive and false negative diagnoses of prostate cancer at multi-parametric prostate MRI in active surveillance. Insights Imaging 2015;6:449-63.

[12] Coker MA, Glaser ZA, Gordetsky JB, Thomas JV, Rais-Bahrami S. Targets missed: predictors of MRI-targeted biopsy failing to accurately localize prostate cancer found on systematic biopsy. Prostate Cancer Prostatic Dis 2018. https://doi.org/10.1038/s41391-018-0062-9.

[13] Lai WS, Zarzour JG, Gordetsky JB, et al. Co-registration of MRI and ultrasound: accuracy of targeting based on radiology-pathology correlation. Transl Androl Urol 2017;6:406-12.

[14] Rosenkrantz AB, Verma S, Choyke P, et al. Prostate magnetic resonance imaging and magnetic resonance imaging targeted biopsy in patients with a prior negative biopsy: a consensus statement by AUA and SAR. J Urol 2016;196:1613-8.

[15] Lai WS, Gordetsky JB, Thomas JV, et al. Factors predicting prostate cancer upgrading on magnetic resonance imaging–targeted biopsy in an active surveillance population. Cancer 2017;123:1941-8.

[16] Gordetsky JB, Saylor B, Bae S, et al. Prostate cancer management choices in patients undergoing multiparametric magnetic resonance imaging/ultrasound fusion biopsy compared to systematic biopsy. Urol Oncol 2018;36:241.e7-241.e13.

[17] Othman E, Wang J, Sprague BL, et al. Comparison of false positive rates for screening breast magnetic resonance imaging (MRI) in high risk women performed on stacked versus alternating schedules. Springerplus 2015;4:77.

[18] Cieszanowski A, Lisowska A, Dabrowska M, et al. MR imaging of pulmonary nodules: detection rate and accuracy of size estimation in comparison to computed tomography. PLoS One 2016;11:e0156272.

[19] Verma S, Turkbey B, Muradyan N, et al. Overview of dynamic contrast-enhanced MRI in prostate cancer diagnosis and management. AJR Am J Roentgenol 2012;198:1277-88.

[20] Djavan B, Zlotta A, Remzi M, et al. Optimal predictors of prostate cancer on repeat prostate biopsy: a prospective study of 1,051 men. J Urol 2000; 163:1144-8.

[21] Keetch DW, Catalona WJ, Smith DS. Serial prostatic biopsies in men with persistently elevated serum prostate specific antigen values. J Urol 1994;151:1571-4.

[22] Hong CW, Walton-Diaz A, Rais-Bahrami S, et al. Imaging and pathology findings after an initial negative MRI-US fusion-guided and 12-core extended sextant prostate biopsy session. Diagn Interv Radiol 2014;20: 234-8.

[23] Liddell H, Jyoti R, Haxhimolla HZ. mp-MRI prostate characterised PIRADS 3 lesions are associated with a low risk of clinically significant prostate cancer—a retrospective review of 92 biopsied PIRADS 3 lesions. Curr Urol 2015;8:96-100.